Research Article | Vol. 29, No. 26 / 20 Dec 2021 / Optics Express 43852
Optics EXPRESS

10-Hz, 636-ps, 1064-nm, all polarization-maintaining fiber front-end based on ultrafast optical fiber pulse chopping

YIZHOU LIU,[1,2,3,4] YI HUA,[1,2] SEDIGHEH MALEK MOHAMADI,[1,2] MIKHAIL PERGAMENT,[1] AND FRANZ X. KÄRTNER[1,2,5,*]

[1]*Center for Free-Electron Laser Science CFEL, Deutsches Elektronen-Synchrotron DESY, Notkestr. 85, 22607 Hamburg, Germany*
[2]*Physics Department, University of Hamburg, Luruper Chaussee 149, Hamburg 22761, Germany*
[3]*School of Information Science and Engineer, Shandong University, Shanda South Road 27, 250100 Jinan, China*
[4]*Key Laboratory of Education Ministry for Laser and Infrared System Integration Technology, Shandong University, Qingdao 266237, China*
[5]*The Hamburg Centre for Ultrafast Imaging, Luruper Chaussee 149, Hamburg 22761, Germany*
[*]*franz.kaertner@desy.de*

Abstract: We demonstrate a robust 10-Hz, 1064-nm, all polarization-maintaining (PM) fiber laser front-end for a joule-level solid-state amplification system applying ultrafast optical pulse chopping. A 1064-nm single frequency continuous wave (CW) laser is chopped by an in-line acousto-optic modulator (AOM) to generate ~7 ns duration pulses at 500-kHz repetition rate, followed by a Sagnac loop (SL) consisting of a 50:50 PM fiber coupler and an electro–optical (EO) phase modulator, which further shortens the pulse duration from 7 ns to 636 ps via a passively fixed optical chopping gate. Finally, the pulse energy is amplified to the sub-μJ level and its repetition rate is further reduced to 10-Hz by another in-line AOM stage. This 10-Hz, 636-ps, sub-μJ level fiber laser realized in an all-PM-fiber configuration can be used as a robust front-end for joule-level solid-state amplification and follow-on nonlinear frequency conversion experiments.

1. Introduction

Rapid improvements in fiber technology over the last decades make highly stable, compact, inexpensive fiber laser systems the most often used laser sources for various applications. Fiber front-end lasers with up to ns-level pulse duration and down to Hz-level repetition rate are attractive in building high pulse energy lasers based on chirped pulse amplification [1–10]. However, fiber front-end system has its own challenges. The combination of a semiconductor saturable absorber mirror (SESAM) and km-scale optical fibers enable the construction of passively mode-locked fiber lasers with kHz-range repetition rate and ns-level pulse duration [11–13]. A further reduction in repetition rate cannot be achieved directly based on this approach limited by its high environmental sensitivity. A combination of MHz-level repetition rate fiber lasers and fiber coupled AOMs can generate low repetition rate pulses [17]. However, mode-locked fiber lasers are inefficient in seeding narrow-bandwidth solid-state amplifiers, such as cryogenic Yb:YAG amplifiers [18]. Narrow-band Q-switched solid-state lasers suffer from large pulse energy fluctuations and beam pointing fluctuations, which limits its applications in high pulse energy amplifiers [19]. Fortunately, ultrafast optical pulse chopping provides a way in generating low repetition rate pulses directly from single-frequency lasers for solid-state amplifiers with narrow gain bandwidth [20]. Utilizing this technique, signal pulses with down to

#445136 https://doi.org/10.1364/OE.445136
Journal © 2021 Received 8 Oct 2021; revised 19 Nov 2021; accepted 26 Nov 2021; published 15 Dec 2021

Optics EXPRESS

ps-level pulse duration can be generated without complicated optical design [14–16]. Therefore, a Hz-level repetition-rate front-end laser generating sub-ns, sub-μJ pulses in an all-PM-fiber configuration based on ultrafast optical pulse chopping can be an ideal front-end laser for high pulse energy solid-state amplifiers.

Ultrafast optical pulse chopping can be used for building a highly stable all-fiber front-end laser with ultra-low repetition rate down to Hz level and ps-scale pulse duration. The fiber front-end can be used to seed high power solid-state amplifiers avoiding temporal long-term drift and beam pointing fluctuations [20–23]. However, the corresponding experimental realization remains to be difficult considering the following effects: (i) amplified spontaneous emission (ASE) [24,25]; (ii) stimulated Brilliouin scattering (SBS) [26,27] and (iii) limitations in the rise time of commercial AOM stages. The ASE can be suppressed by optical-gating with the AOM stage and spectral filtering, while the SBS can be managed by controlling optical parameters of the fiber amplifiers. However, the ns-level rise time of commercial fiber-coupled AOMs limits the possibilities in directly generating ps-level pulses via optical pulse chopping. Therefore, there are urgent requirements for investigating a new ultrafast optical pulse chopping method for generating ps-level pulses.

In this paper, we investigate an ultrafast optical pulse chopping method by utilizing a combination of a GHz-level bandwidth EO phase modulator and an all-PM-fiber Sagnac Loop [28,29]. This optical pulse chopper can build a passively fixed temporal gate generating stable ps-scale pulses with >20 dB contrast ratio. Specifically, a 10-Hz repetition rate, 1064-nm, all-PM-fiber front-end laser with 636-ps pulse duration and 360-nJ pulse energy is built as a seeder for a 2-J Nd:YAG laser amplifier. In section 2, we introduce the schematic layout and experimental results of this ps-scale optical pulse chopper. In section 3, we describe the construction and experimental results of the complete 10-Hz, 636-ps, 360-nJ, 1064-nm, all-PM-fiber front-end laser system. Conclusions are discussed in section 4.

2. Picosecond-duration optical pulse chopper with passively fixed temporal gate

Optical pulse choppers built with AOMs have nanosecond-level rise times. Therefore, AOMs have restrictions in realizing picosecond-duration optical pulses. Previous designs consisted of long non-polarization maintaining fiber forming a Sagnac loop and an EO phase modulator in/outside the loop [30–32]. These designs show instabilities when compared with the all-PM-fiber construction and work mostly for high-repetition-rate applications. Nevertheless, there is still a lack of robust and easy to implement low repetition rate, ps-duration, all-PM-fiber front-end lasers applying the ultrafast optical pulse chopping. Here, we demonstrate for the first time to our knowledge, an all-PM-fiber, optical pulse chopper with ps-duration rise and fall times and passively fixed temporal gate, which can generate flat-top optical pulses. It is a combination of a PM fiber EO phase modulator and the 2×2, 50:50 PM fiber coupler.

Figure 1 shows the schematic design of the ps-duration ultrafast optical pulse chopper. The EO phase modulator with PM pigtails is spliced asymmetrically with the 50:50 PM fiber coupler to introduce a π phase difference to counter-propagating beams by the EO phase modulator and to ensure generation of a temporal gate at the transmission port of the 50:50 coupler. The optical path difference of these two counter-propagating beams inside the all-PM fiber SL determines the temporal width of the optical chopping gate.

The SL can be modelled as a Mach-Zehnder interferometer (MZI) for further analysis as shown in Fig. 2(a). Input and output beam splitters of the MZI correspond to the 50:50 coupler in the SL shown in Fig. 1. The phase of the clock-wise and counter clock-wise propagating beams can be visualized as φ_{CW} and φ_{CCW}. These two EO phase modulators correspond to the single EO phase modulator inside the asymmetric SL. There is a π phase bias added to counter-propagating beams at T_0 right after coupling the modulated RF signal into the EO phase modulator. The

Optics EXPRESS

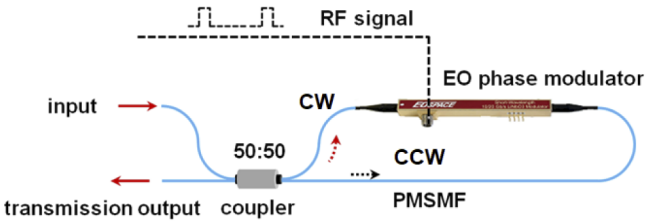

Fig. 1. Schematic design of the picoseconds-level ultrafast optical pulse chopper. CCW: counter clock-wise, CW: clock-wise.

orange area in Fig. 2(a) illustrates the rise time area of the EO phase modulator. Therefore, the temporal range gathering the π phase bias for φ_{CW} and φ_{CCW} is caused by the asymmetric location of the EO phase modulator inside the SL. Therefore, a temporal gate ΔT can be generated at the transmission port (the output port illustrated in Fig. 2). The width of the temporal gate can be calculated applying Eq. (1)–(3), where $\tau_T = n|L_{right} - L_{left}|/c$ is the temporal window determined by the pigtails length difference, n is the refractive index of fiber, c is the speed of light, $|L_{left} - L_{right}|$ is the corresponding pigtails length difference of the EO phase modulator, and τ_R is the rise time of the EO phase modulator.

$$\begin{cases} \Delta T = \tau_T - \tau_R + \dfrac{2\tau_R}{2} = \tau_T, & \tau_T \geq \tau_R \quad (1) \\ \Delta T = \tau_R - \tau_T + \dfrac{2\tau_T}{2} = \tau_R, & 0 < \tau_T < \tau_R \quad (2) \\ \Delta T = 0, & \tau_T = 0 \quad (3) \end{cases}$$

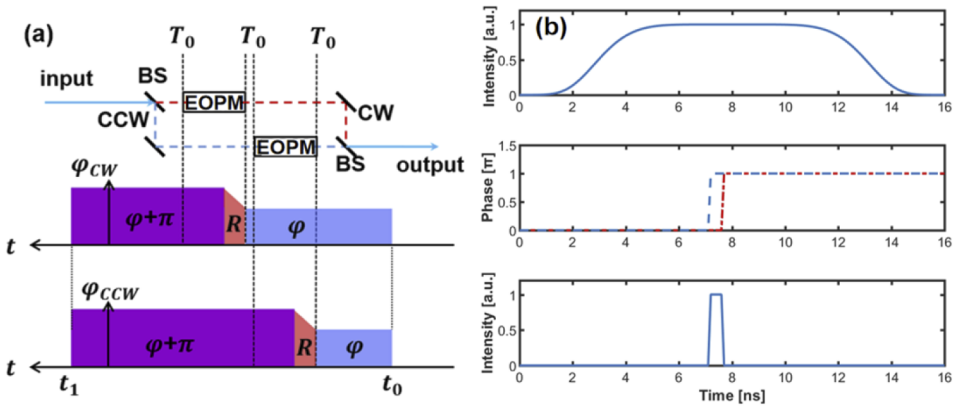

Fig. 2. Temporal illustration (a) and simulation results (b) of the SL pulse chopper. CCW: counter clock-wise, CW: clock-wise, BS: beam splitter, EOPM: eletro-optical phase modulator.

Figure 2(b) shows numerical simulation results by inputting a 10-ns pulse into this optical pulse chopper. There is the π phase bias for counter-propagating beams generating a picosecond-duration pulset the transmission port of the SL. The 100-ps rise time of the EO phase modulator shown in the picture in the middle of Fig. 2(b) determines the front-edge of the output pulse as shown in the picture at the bottom of Fig. 2(b). Therefore, it is clear that a flat-top pulse with picosecond pulse duration can be generated applying this method. The pulse duration is limited by the rise time of the EO phase modulator.

Optics EXPRESS

Experiments were performed to prove the simulation results by inputting a flat top optical pulse with ~7 ns pulse duration into this optical pulse chopper. The length difference between these two pigtails was set to be ~12 cm aiming to achieve chopped pulses with ~600 ps pulse duration. The black curve in Fig. 3 shows the ultrafast chopping results. The pulse duration was shortened to ~636 ps. The coupling ratio of the 50:50 optical coupler is 49.94242:50.05758 indicating the signal to noise ratio is >40 dB. An ultrafast rise time module DG645 (Stanford Research Systems, SRS) was used to provide the driving RF signal with ~100 ps rise time for the EO phase modulator (EOSPACE). The bandwidth of the EO phase modulator is 10 GHz corresponding to ~10 ps rise time, which is about 10% of the EO response time. Therefore, the final rise time of the optical pulse chopping process is limited by the RF signal with a longer rise time. Obviously, the pulse width of the chopped pulse can be tuned by changing the fiber length difference $|L_{left} - L_{right}|$, when $\tau_T \geq \tau_R$. Further shorter pulses with >100-ps pulse duration can be simply generated by shortening the fiber length difference. Chopped pulses with <100-ps pulse duration can also be generated applying a RF driving signal with <100-ps rise time, when $0<\tau_T<\tau_R$.

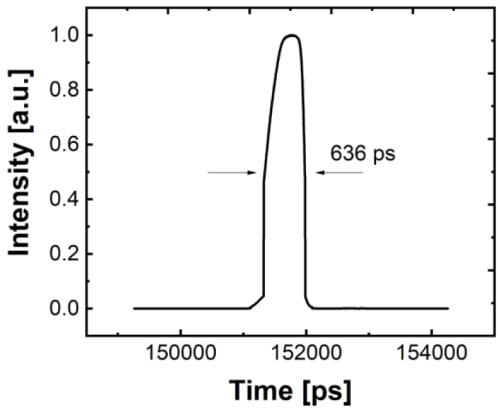

Fig. 3. 636-ps pulse profile chopped by the SL from a 7-ns signal pulse. The asymmetric profile is caused by the transfer function of the photo detector.

3. 10-Hz, 636-ps, 360-nJ, 1064-nm, all PM fiber front-end

Figure 4 shows the schematic layout of the 10-Hz, 636-ps, 360-nJ, 1064-nm, all-PM-fiber front-end using the ultrafast optical pulse chopper as the key module to generate ps-duration pulses. This system consists of two AOM stages and an ultrafast optical pulse chopping stage. Cascaded PM fiber amplifiers are employed before the chopping stages to pre-compensate their insertion loss. The seed source of the system is a single frequency 1064-nm CW laser with 2-MHz bandwidth and 40-mW maximum output power. The 1064-nm CW laser is amplified to 300 mW by two cascaded PM fiber amplifiers that consist of a polarization maintaining wavelength division multiplexer (PMWDM), a PM fiber isolator and 0.5-m ytterbium doped gain fiber (YB 401-PM). The first AOM with <3 dB item insertion loss (Gooch&Housego) creates a pulse train with 500 kHz repetition rate for the next chopping stage. The pulse duration of the pulses is ~7 ns. This <10-ns pulse width was chosen to avoid potential SBS effects in subsequent fiber amplifiers considering the 100-MHz intrinsic gain bandwidth of the Brillouin gain of the fused silica. The average output power of the 500-kHz laser is ~1.5 mW. We used a 1064-nm bandpass filter with 2-nm bandwidth inserted between these two cascaded PM fiber amplifiers to suppress the ASE.

Optics EXPRESS

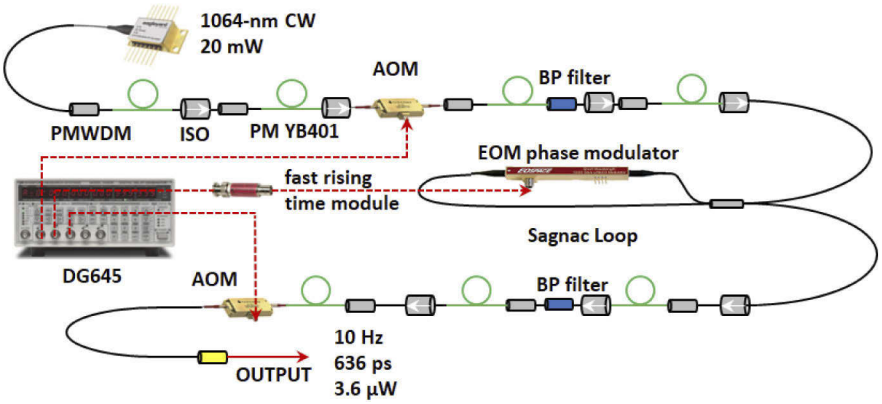

Fig. 4. Schematic layout of the 10-Hz, 636-ps, 360-nJ, 1064-nm, all PM fiber laser front-end.

The 500-kHz pulse train is further amplified to 95 mW just below the 100-mW optical damage threshold of the EO phase modulator installed into the SL. The length difference between these two PM pigtails of the EO phase modulator is cut to ~12 cm. Therefore, the optical chopping gate of the ultrafast optical pulse chopper is set to ~600 ps and carefully located within the central area of the 7-ns input pulse by moderating the delay of the RF modulation signal from the DG645. The pulse width of the chopped signal pulse is decreased from 7 ns to 636 ps by this ultrafast optical pulse chopper. Because the rise time of the EO phase modulator is ~100 ps, the chopped pulse width can be shorter via decreasing the fiber length difference. The average power of the output signal laser after the SL stage is ~1.5 mW. There is one more 1064-nm bandpass filter spliced after the 5th PM fiber amplifier to supress the ASE generated during the signal amplification. The gain fiber length of the 7th PM fiber amplifier is set to be 75 cm. It is 1.5 times longer than the gain fiber (Yb 401-PM) length utilized in front PM fiber amplifiers. Therefore, the residual generated 1030-nm ASE can be absorbed by this 75-cm highly-doped gain fiber.

The second AOM reduced the repetition rate from 500 kHz to 10 Hz and also contributed to a reduction of ASE in improving the signal to noise ratio. The final output pulse energy of the 10-Hz laser can be amplified up to ~1 μJ by adding an additional 8th PM fiber amplifier before the second AOM stage, taking into account the 1-W average power damage threshold of the AOM crystal. However, we keep the output pulse energy to be ~360 nJ, which is sufficient to seed the follow on high pulse energy solid-state amplifiers.

Figure 5 shows the spectra of the single frequency, 1064.25-nm seeder (black curve) and the 10-Hz, output pulse (red curve, 0.08-nm spectral bandwidth) in linear scale. The measured spectra are limited by the resolution of the spectrum analyzer (Ando, AQ-6315A), which is about 0.05 nm. The linewidth of the single frequency seeder is 2 MHz. The central wavelength of the single frequency laser can be tuned from ~1064.15 nm to ~1064.35 nm by modifying the working temperature and current of the laser diode. The temperature coefficient for wavelength tuning is 0.06 nm/K. The current coefficient is 0.003 nm/mA.

Stability characteristics of the resulting 10-Hz front-end laser were also measured and are demonstrated in Fig. 6. The wavelength stability of the 1064-nm seed laser driven by CLD1015 (Thorlabs) is shown in Fig. 6(a) measured at 10 °C working temperature. The central wavelength of the 1064-nm seed laser stays the same after 10 minutes warming up time. Figure 6(b) shows the output power stability of the 1064-nm seed laser. Figure 6(c) shows the standard deviation of the 10-Hz output pulses, which is 1.13 nJ for 103 nJ output pulse energy. The inset shows the perfect near-field beam profile of the all-PM-fiber front-end laser. Figure 6(d) shows the

Optics EXPRESS

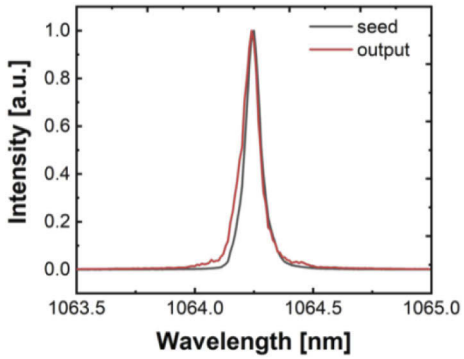

Fig. 5. Spectra of the 1064-nm CW seeder (black curve) and the output 10-Hz laser (red curve) in linear scale.

measured repetition rate fluctuation of the output laser using the internal clock of the DG645 as a reference. The average fluctuation was <1 mHz based on a 2-hour measurement.

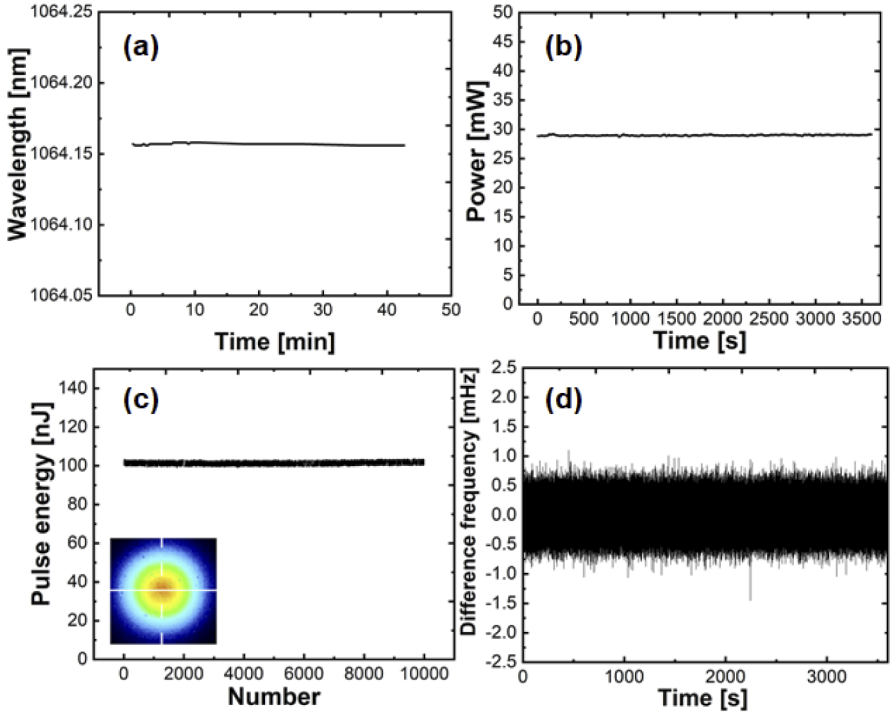

Fig. 6. (a) the wavelength stability of the 1064-nm seeder; (b) the output power stability of the 1064-nm seeder; (c) the output pulse energy stability of the system; (d) the output repetition rate fluctuation at 500 kHz after locking the counter with the internal reference clock of the DG645.

4. Conclusion

We have demonstrated a 10-Hz, 360-nJ, 636-ps, 1064-nm all-PM-fiber front-end for seeding of 2-J solid state amplification system. The ultra-low repetition rate of the front-end laser controlled

Optics EXPRESS

by the AOM is tunable and the pulse energy of the final output can be scaled up to 1 μJ depending on applications. An ultrafast all-PM-fiber optical pulse chopper consisted of a PM fiber EO phase modulator and a 50:50 PM fiber coupler used in the construction of a Sagnac loop achieves optical pulses with ps-level pulse duration. There is one AOM chopping stage generating 500-kHz, 7-ns pulses to avoid the potential influence of SBS effects in subsequent fiber amplifiers. There is another AOM stage used to tune the repetition rate of the output laser from 500-kHz to hertz-level or even lower repetition rate and remove the residual ASE generated from the last three fiber amplifiers. The 1064-nm bandpass filter with 2-nm bandwidth and 75-cm highly doped gain fiber of the 7th PM fiber amplifier are also used to inhibit the ASE generated during the amplification process.

This ultrafast all-PM-fiber optical pulse chopper provides a robust, inexpensive, and sufficient way in generating ultrashort pulses with passively fixed ps-level pulse duration and sub-μJ level pulse energy to seed joule-class solid-state amplifiers.

Funding. European Research Council (609920); Helmholtz Association; Deutsches Elektronen-Synchrotron; China Scholarship Council.

Acknowledgments. The authors acknowledge many helpful discussions with Dr. Yuxuan Ma and Dr. Wenlong Tian.

Disclosures. The authors declare that there are no conflicts of interest related to this article.

Data availability. Data underlying the results presented in this paper are not publicly available at this time but can be obtained from the authors upon reasonable request.

References

1. P. Maine, D. Strickland, P. Bado, M. Pessot, and G. Mourou, "Generation of ultrahigh peak power pulses by chirped pulse amplification," IEEE J. Quantum Electron. **24**(2), 398–403 (1988).
2. F. Röser, T. Eidam, J. Rothhardt, O. Schmidt, D. N. Schimpf, J. Limpert, and A. Tünnermann, "Millijoule pulse energy high repetition rate femtosecond fiber chirped-pulse amplification system," Opt. Lett. **32**(24), 3495–3497 (2007).
3. S. Tokita, J. Kawanaka, M. Fujita, T. Kawashima, and Y. Izawa, "Efficient High-Average-Power Operation of Q-Switched Cryogenic Yb:YAG Laser Oscillator," Jpn. J. Appl. Phys. **44**(No. 50), L1529–L1531 (2005).
4. K. Furuta, T. Kojima, S. Fujikawa, and J. Nishimae, "Diode-pumped 1 kW Q-switched Nd:YAG rod laser with high peak power and high beam quality," Appl. Opt. **44**(19), 4119–4122 (2005).
5. I. Freitag, A. Tünnermann, and H. Welling, "Passively Q-switched Nd:YAG ring lasers with high average output power in single-frequency operation," Opt. Lett. **22**(10), 706–708 (1997).
6. F. Friebel, F. Druon, J. Boudeile, D. N. Papadopoulos, M. Hanna, P. Georges, P. Camy, J. L. Doualan, A. Benayad, R. Moncorgé, C. Cassagne, and G. Boudebs, "Diode-pumped 99 fs Yb:CaF_2 oscillator," Opt. Lett. **34**(9), 1474–1476 (2009).
7. A. Chong, J. Buckley, W. Renninger, and F. Wise, "All-normal-dispersion femtosecond fiber laser," Opt. Express **14**(21), 10095–10100 (2006).
8. O. Pronin, J. Brons, C. Grasse, V. Pervak, G. Boehm, M.-C. Amann, V. L. Kalashnikov, A. Apolonski, and F. Krausz, "High-power 200 fs Kerr-lens mode-locked Yb:YAG thin-disk oscillator," Opt. Lett. **36**(24), 4746–4748 (2011).
9. D. H. Sutter, G. Steinmeyer, L. Gallmann, N. Matuschek, F. Morier-Genoud, U. Keller, V. Scheuer, G. Angelow, and T. Tschudi, "Semiconductor saturable-absorber mirror-assisted Kerr-lens mode-locked Ti:sapphire laser producing pulses in the two-cycle regime," Opt. Lett. **24**(9), 631–633 (1999).
10. S. Yang and X. Bao, "Generating a high-extinction-ratio pulse from a phase-modulated optical signal with a dispersion-imbalanced nonlinear loop mirror," Opt. Lett. **31**(8), 1032–1034 (2006).
11. S. Kobtsev, S. Kukarin, and Y. Fedotov, "Ultra-low repetition rate mode-locked fiber laser with high-energy pulses," Opt. Express **16**(26), 21936–21941 (2008).
12. M. Zhang, L. Chen, C. Zhou, Y. Cai, L. Ren, and Z. Zhang, "Mode-locked ytterbium-doped linear-cavity fiber laser operated at low repetition rate," Laser Phys. Lett. **6**(9), 657–660 (2009).
13. L. Kong, X. Xiao, and C. Yang, "Low-repetition-rate all-fiber all-normal-dispersion Yb-doped mode-locked fiber laser," Laser Phys. Lett. **7**(5), 359–362 (2010).
14. J.-K. Rhee, T. S. Sosnowski, T. B. Norris, J. A. Arns, and W. S. Colburn, "Chirped-pulse amplification of 85-fs pulses at 250 kHz with third-order dispersion compensation by use of holographic transmission gratings," Opt. Lett. **19**(19), 1550–1552 (1994).
15. P. S. Banks, M. D. Perry, V. Yanovsky, S. N. Fochs, B. C. Stuart, and J. Zweiback, "Novel all-reflective stretcher for chirped-pulse amplification of ultrashort pulses," IEEE J. Quantum Electron. **36**(3), 268–274 (2000).
16. G. Imeshev, I. Hartl, and M. E. Fermann, "Chirped pulse amplification with an nonlinearly chirped fiber Bragg grating matched to the Treacy compressor," Opt. Lett. **29**(7), 679–681 (2004).

Optics EXPRESS

17. Y. Liu, P. Krogen, K.-H. Hong, Q. Cao, P. Keathley, and F. X. Kärtner, "Fiber-amplifier-pumped, 1-MHz, 1-μJ, 2.1-μm, femtosecond OPA with chirped-pulse DFG front-end," Opt. Express **27**(6), 9144–9154 (2019).
18. D. J. Ripin, J. R. Ochoa, R. L. Aggarwal, and T. Y. Fan, "300-W cryogenically cooled Yb:YAG laser," IEEE J. Quantum Electron. **41**(10), 1274–1277 (2005).
19. R. Beach, J. Davin, S. Mitchell, W. Benett, B. Freitas, R. Solarz, and P. Avizonis, "Passively Q-switched transverse-diode-pumped Nd^{3+}:YLF laser oscillator," Opt. Lett. **17**(2), 124–126 (1992).
20. P. Wan, J. Liu, L.-M. Yang, and F. Amzajerdian, "Low repetition rate high energy 1.5 μm fiber laser," Opt. Express **19**(19), 18067–18071 (2011).
21. M. Ostermeyer, P. Kappe, R. Menzel, and V. Wulfmeyer, "Diode-pumped Nd:YAG master oscillator power amplifier with high pulse energy, excellent beam quality, and frequency-stabilized master oscillator as a basis for a next-generation lidar system," Appl. Opt. **44**(4), 582–590 (2005).
22. J. Tümmler, R. Jung, H. Stiel, P. V. Nickles, and W. Sandner, "High-repetition-rate chirped-pulse-amplification thin-disk laser system with joule-level pulse energy," Opt. Lett. **34**(9), 1378–1380 (2009).
23. J. Hein, S. Podleska, M. Siebold, M. Hellwing, R. Bödefeld, R. Sauerbrey, D. Ehrt, and W. Wintzer, "Diode-pumped chirped pulse amplification to the joule level," Appl. Phys. B **79**(4), 419–422 (2004).
24. G. Haag, M. Munz, and G. Marowsky, "Amplified spontaneous emission (ASE) in laser oscillators and amplifiers," IEEE J. Quantum Electron. **19**(6), 1149–1160 (1983).
25. O. D. Vries, M. Plötner, F. Christaller, H. Zhang, A. Belz, B. Heinrich, H. Kübler, R. Löw, T. Pfau, T. Walbaum, T. Schreiber, and A. Tünnermann, "Highly customized 1010 nm, ns-pulsed Yb-doped fiber amplifier as a key tool for on-demand single-photon generation," Opt. Express **28**(12), 17362–17373 (2020).
26. K. Shiraki, M. Ohashi, and M. Tateda, "SBS threshold of a fiber with a Brillouin frequency shift," J. Lightwave Technol. **14**(1), 50–57 (1996).
27. W. Shi, E. B. Petersen, Z. Yao, D. T. Nguyen, J. Zong, M. A. Stephen, A. Chavez-Pirson, and N. Peyghambarian, "Kilowatt-level stimulated-Brillouin-scattering-threshold monolithic transform-limited 100 ns pulsed fiber laser at 1530 nm," Opt. Lett. **35**(14), 2418–2420 (2010).
28. M. L. Dennis, I. N. Duling, and W. K. Burns, "Sagnac interferometer amplitude modulator," Summaries of papers presented at *the Conference on Lasers and Electro-Optics*, Anaheim, CA, USA, 331–332 (1996).
29. S. Datta and B. Das, "Electronic analog of the electro-optic modulator," Appl. Phys. Lett. **56**(7), 665–667 (1990).
30. O. Tarasenko and W. Margulis, "Electro-optical fiber modulation in a Sagnac interferometer," Opt. Lett. **32**(11), 1356–1358 (2007).
31. K. Wada, S. Takamatsu, H. Watanabe, T. Matsuyama, and H. Horinaka, "Pulse-Shaping of gain-switched pulse from multimode laser diode using fiber Sagnac interferometer," Opt. Express **16**(24), 19872–19881 (2008).
32. O. G. Okhotnikov and F. M. Araújo, "Cavity dumping of fiber lasers by phase-modulated optical loop mirrors," Opt. Lett. **21**(1), 57–58 (1996).